Kinetic mechanisms and species densities in N2/(0–5%)H2 afterglows

Valentin Ferrer, André Ricard, J P Gardou, Frédéric Marchal, J. Amorim, Jean-Philippe Sarrette

Journal Pre-proofs

Kinetic mechanisms and species densities in N_2/(0–5%)H_2 afterglows

V. Ferrer, A. Ricard, J.P. Gardou, F. Marchal, J. Amorim, J.P. Sarrette

PII: S0009-2614(24)00016-2
DOI: https://doi.org/10.1016/j.cplett.2024.141079
Reference: CPLETT 141079

To appear in: *Chemical Physics Letters*

Received Date: 7 September 2023
Revised Date: 14 December 2023
Accepted Date: 9 January 2024

Please cite this article as: V. Ferrer, A. Ricard, J.P. Gardou, F. Marchal, J. Amorim, J.P. Sarrette, Kinetic mechanisms and species densities in N_2/(0–5%)H_2 afterglows, *Chemical Physics Letters* (2024), doi: https://doi.org/10.1016/j.cplett.2024.141079

Kinetic mechanisms and species densities in N_2/(0-5%)H_2 afterglows

V.Ferrer[1], A. Ricard[1], J.P. Gardou[1], F. Marchal[1], J. Amorim[2] and J.P. Sarrette[1]

[1]Université de Toulouse ; UPS, INP ; LAPLACE (Laboratoire Plasma et Conversion d'Energie) ; 118 route de Narbonne, F-31062 Toulouse, France

[2]Departamento de Física, Instituto de Ciências Exatas-ICEx, Universidade Federal Fluminense, Campus do Aterrado, Volta Redonda, Rio de Janeiro 27213-145, Brazil

Abstract

N atoms absolute concentrations were obtained in the afterglows of N_2/(x=0-5%H_2) mixtures by optical emission spectroscopy (OES) coupled with NO titration in the 2-6 Torr pressure range and at distances to the discharge varying between 20 and 50 cm. Band intensity measurements were then used to obtain absolute concentrations of N_2(A) and N_2(X, v>13) metastable molecules in the same conditions. From these data, absolute NH and H-atoms densities were deduced from a set of kinetic mechanisms. Independently, absolute N and H atoms densities were also measured using the TALIF technique. The comparison between TALIF and OES results suggests that the NH species can be generated outside the discharge (i.e. in the afterglow) by the 3-body recombination process $N + H + N_2 \rightarrow NH + N_2$, with a rate coefficient of 1.0 10^{-33} cm^6 s^{-1}, the NH(A) state being itself produced by the reaction $N_2(X,v > 13) + NH \rightarrow NH(A) + N_2$, with a rate equal to 5 10^{-11} cm^3 s^{-1}. The agreement between the TALIF and OES measurements is further improved considering the role of N(^{2}D) metastable atoms in the H and NH kinetics.

1 – Introduction

Previous results [1,2] have reported that the introduction of a small H_2 quantity, less than 1%, into N_2 and Ar-N_2 microwave discharges produced a marked increase of the N and H-atom densities in the afterglows flowing at reduced pressure (2-20 Torr). Several studies of the electron and vibrational kinetics of N_2-H_2 discharges [3,4,5] have also concluded to an increase of the electron energy and thus of the electron excitation and dissociation of N_2 and H_2 as a few H_2 was introduced into N_2.

In this work, the H-atom density present in N_2/(0-5%)H_2 flowing afterglows was determined by two independent methods. The first one is Optical Emission Spectroscopy (OES), easy to experimentally overcome with a standard spectrometer but based on a simplification of the kinetics reactions populating and depopulating the emitting states and requiring the knowledge of the associated rate coefficients. The second method is Two-Photon Absorption Laser Induced Fluorescence (TALIF), more complex to implement but allowing obtaining after calibration the absolute H-atom density without any kinetic assumption. These two methods are here used and compared to validate both the kinetic scheme populating the emitting NH(A) state from which the H-atom density is obtained in the flowing afterglow and to choose the most appropriate rate coefficients from data available in the literature.

2 – Experimental set-up

Figure 1 shows a photography of the experimental set-up. The plasma is produced by a microwave surfatron launcher (2.45 GHz, 50-200 W) in gas mixtures flowing in a 4 mm i.d. quartz discharge tube. The different gas flow rates are separately controlled by flow-meters in the 0.3-3.0 slm range. At 10 cm downstream the surfatron gap, the discharge tube enlarges to a second quartz tube of 19 mm i.d. and 60 cm in length, itself connected to a 5 liters pyrex reactor. Three different tubes can be mounted, each equipped with a pair of symmetrical MgF_2 windows (Fig. 1) allowing the laser beam to cross perpendicularly the afterglow flow. MgF_2 windows were installed at z = 20, 30 or 50 cm from the discharge, allowing performing TALIF measurements at different positions in the afterglow. The operating pressure can be adjusted between 2 and 20 Torr by means of a throttle valve and a rotary vane pump placed downstream the reactor.

Emission spectra were recorded perpendicularly from the tube axis by a mobile optical fiber connected to an Acton Spectra Pro 2500i spectrometer (focal length 50 cm, grating 600 gr/mm) equipped with a front illuminated Pixis 256E CCD detector (1024 x 256 pixels).

Detailed informations concerning the TALIF set-up and the TALIF signal calibration by Krypton were given in [6]. The two-photon excitation and fluorescence schemes used for the detection of N and H atoms and for Kr calibration are shown Figure 2. The tunable UV laser beam (206.65 nm for N, 205.08 nm for H or 204.13 nm for Kr) was focused by a MgF_2 250 mm focal length lens at the center of the afterglow tube and the fluorescence signal emitted by the afterglow was focused and collected perpendicularly to the afterglow axis by a Hamamatsu H7421-50 photomultiplier operating in photon counting mode. As time (Δt = 0.512 ns) and wavelength ($\Delta\lambda$ = 1 pm) resolved photon counting were performed, the TALIF fluorescence intensity was obtained by integrating the wavelength signal over the whole laser excitation profile while the temporal fluorescence signal variation provides the radiative lifetime of the excited state and then the effect of quenching on the excited state population.

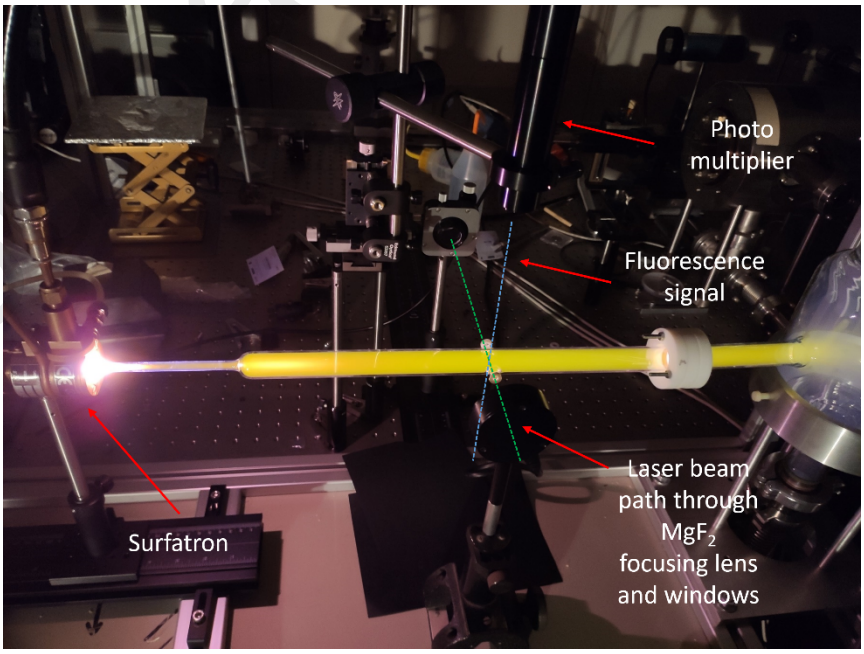

Fig.1. Photography of the experimental set-up showing the afterglow operating in pure N_2, the laser beam path through the MgF_2 lens and windows and the photomultiplier collecting the fluorescence signal.

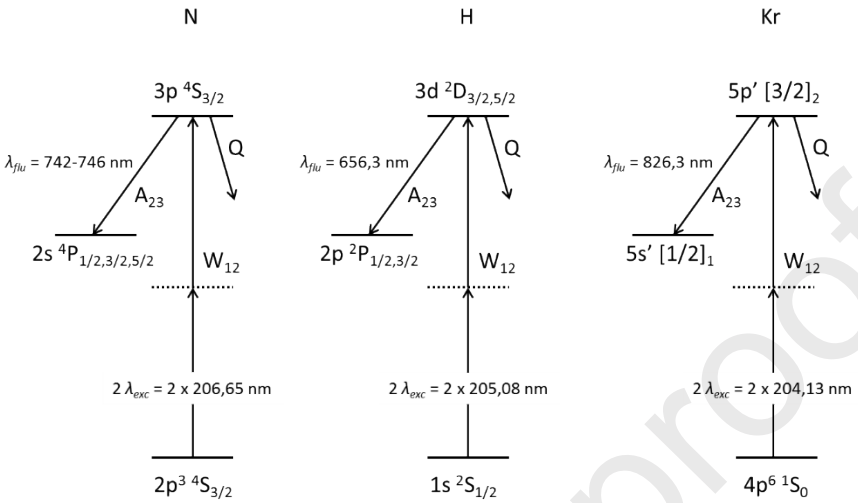

Fig.2. Two-photon excitation and fluorescence schemes of N, H and Kr (calibration) used in this work.

3 – Determination of N-atoms and of N_2(A) and N_2(X, v>13) metastable molecules absolute densities using band intensity ratios

As can be seen on Figure 1 and on the spectra presented Figure 3, emission in the late afterglow region (z = 50 cm) of N_2/(x=0-5%H_2) mixtures is dominated by the N_2 first positive (1+) N_2(B,v'=11) → N_2(A,v''=7) vibrational transition, conducing to an intense yellow-green emission at 580 nm (I_{580nm}^{11-7}).

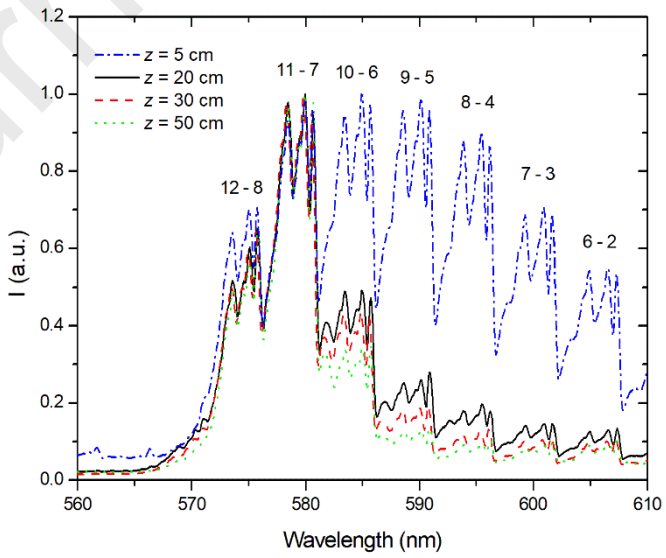

Fig.3. Emission spectra of the N_2 1+ Δv = 4 sequence recorded in a N_2/1%H_2 afterglow at different distances z to the discharge. Spectra are normalized to the maximum emission of the N_2 1+ (11-7) band at 580 nm.

(4 Torr, 0.5 slm, 150 W)

In this late afterglow region, the N_2(B,v'=11) level is only produced by the N-atom 3-body recombination :

$$N + N + N_2 \rightarrow N_2(B,v' = 11) + N_2, \quad \text{(a)}$$

and we have:

$$I_{580nm}^{11-7} = K' \left[N_2(B,v' = 11)\right] = K^{580}\,[N]^2. \quad (1)$$

The NO titration method, presented in detail in [7], allows obtaining the absolute N-atom density and the proportionality constant K^{580} relating it to the observed band intensity I_{580nm}^{11-7}.

Closer to the discharge (*z* = 20 or 30 cm), concentrations of high vibrational levels N_2(X,v'>13) and of N_2(A) metastable states are still high and the full afterglow condition is not obligatory fulfilled as the N_2(B,v'=11) level can also be significantly populated by reaction (b) ([8], [9]):

$$N_2(X,v' > 13) + N_2(A) \rightarrow N_2(B,v' = 11) + N_2, \quad \text{(b)}$$

implying that only a fraction *a* (0 < *a* ≤ 1, where *a* = 1 stands for full late afterglow conditions) of the observed I_{580nm}^{11-7} intensity can be related with $[N]^2$:

$$a\, I_{580nm}^{11-7} = K^{580}\,[N]^2. \quad (2)$$

In the full pink afterglow region (*z* = 5 cm), the population mechanisms of the N_2(B,v'=11) level are dominated by reaction (b), conducing to *a* = 0.

The value of the *a* fraction at a given observation point *z* in the afterglow for a given set of operating parameters (pressure, total gas flow rate, microwave power, gas mixture) can be obtained [10] by observing the changes in the vibrational band intensity distribution of the Δ*v* = 4 sequence of the N_2 1+ system between the full pink (*a* = 0) and the full late (*a* = 1) regions of the afterglow (Fig. 3), and considering the relation:

$$I_{580nm}^{11-7}(z) = a\, I_{580nm}^{11-7}(z = 50\ cm) + (1 - a)\, I_{580nm}^{11-7}(z = 5\ cm). \quad (3)$$

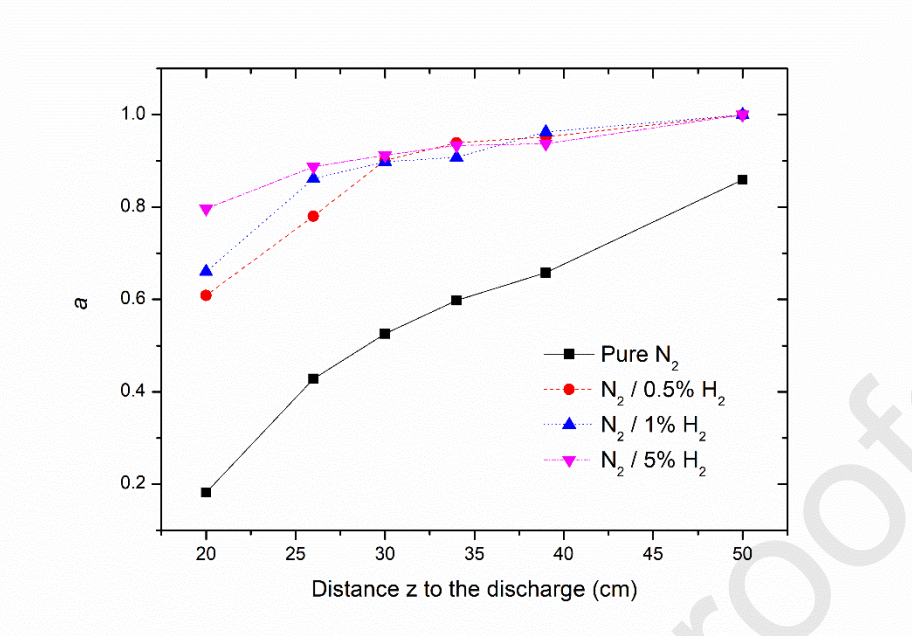

Fig.4. Variation of the a fraction with the distance z to the discharge in different N_2/(0-5%H_2) mixtures. (4 Torr, 0.5 slm, 150 W)

Figure 4 shows the variations of the *a* fraction obtained along the afterglows in pure N_2 and in the different N_2/H_2 mixtures studied in this work (4 Torr, 0.5 slm, 150 W). It is observed that for these operating conditions, a full late afterglow (a = 1) is not yet reached at z = 50 cm from the discharge in pure N_2, the *a* fraction varying almost linearly between z = 20 and z = 50 cm. In N_2/H_2 mixtures, as the *a* fraction is always higher than 0.6, it is deduced that reaction (a) is the main population mechanism of the N_2(B,v'=11) level in the afterglow at distances higher than 20 cm from the discharge, the full late afterglow condition being always obtained at z = 50 cm.

Once the *a* value obtained at a given *z* position, the absolute N-atom density is deduced from the measured $I_{580\mathrm{nm}}^{11-7}(\mathrm{z})$ band intensity through eq. (2). From a practical point of view, as bands overlap within the N_2 1+ Δv = 4 sequence (Figure 3), half of the measured I^{10-6} band intensity at 581 nm (wavelength where the (11-7) and the (10-6) bands overlap) is subtracted to the measured maximum intensity of the (11-7) band.

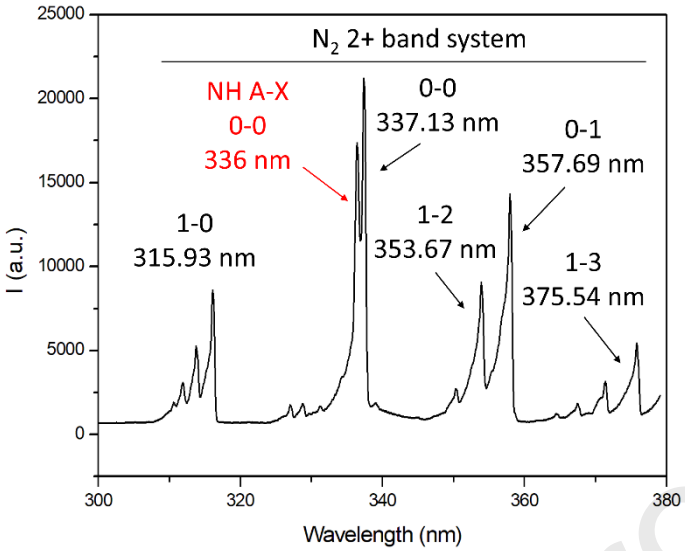

Fig.5. Emission spectra recorded at z = 30 cm from the surfatron gap in the afterglow of a N_2/1%H_2 mixture at 2 Torr (0.5 slm, 150 W).

Figure 5 presents the emission spectra recorded in the UV-A region at *z* = 30 cm from the surfatron gap in the afterglow of a N_2/1%H_2 mixture (2 Torr, 0.5 slm, 150 W), showing different bands of the N_2 2+ system emitted by the N_2(C,v'=0,1) levels. Among these bands, the N_2 2+ (1-0) at 316 nm is well separated from the others and was used to obtain the N_2(A) absolute density.

The method, already exposed in refs [6], [8] and [9], is based on the assumption that reaction (c):

$$N_2(A) + N_2(A) \rightarrow N_2(C,v' = 1) + N_2(X) \qquad \text{(c)}$$

is the dominant production mechanism of the N_2(C,v'=1) level at the origin of the N_2 2+ (1-0) emission at 316 nm.

In this condition, the observed band intensity ratio $\frac{a\, I_{580nm}^{11-7}}{I_{316nm}^{1-0}}$ evolves as:

$$\frac{a\, I_{580nm}^{11-7}}{I_{316nm}^{1-0}} = \frac{K^{580}\,[N]^2}{K^{316}\,[N_2(A)]^2}. \qquad (4)$$

Using the quasi-stationarity assumption, the K^{580} and K^{316} constants can be analytically expressed as :

$$I_{580nm}^{11-7} = C(580nm) \cdot \frac{hc}{580nm} \cdot A_{N_2(\mathrm{A},v''=7)}^{N_2(\mathrm{B},v'=11)} \cdot [N_2(B,v' = 11)] \qquad (5)$$

$$a\, I_{580nm}^{11-7} = C(580nm) \cdot \frac{hc}{580nm} \cdot A_{N_2(\mathrm{A},v''=7)}^{N_2(\mathrm{B},v'=11)} \cdot \frac{k_a[N]^2}{\nu_{N_2(B,11)}^{R} + [N_2]k_{N_2(B,11)}^{Q_{N_2}} + [H_2]k_{N_2(B,11)}^{Q_{H_2}}} = K^{580}\,[N]^2 \qquad (6)$$

and

$$I_{316nm}^{1-0} = C(316nm) \cdot \frac{hc}{316nm} \cdot A_{N_2(\mathrm{B},v''=0)}^{N_2(\mathrm{C},v'=1)} \cdot [N_2(C,v' = 1)] \qquad (7)$$

$$I_{316nm}^{1-0} = C(316nm) \cdot \frac{hc}{316nm} \cdot A_{N_2(\mathrm{B},v''=0)}^{N_2(\mathrm{C},v'=1)} \frac{k_c[N_2(A)]^2}{\nu_{N_2(C,1)}^R + [N_2]k_{N_2(C,1)}^{Q_{N_2}} + [H_2]k_{N_2(C,1)}^{Q_{H_2}}} = K^{316}\,[N_2(A)]^2. \qquad (8)$$

In these equations, $C(\lambda)$ is the spectral response of the whole intensity acquisition system, obtained in arbitrary unit with a deuterium-tungsten halogen source (Ocean Optics DH-3P-BAL-CAL), $A_{N_2(\mathrm{A},v''=7)}^{N_2(\mathrm{B},v'=11)}$ and $\nu_{N_2(B,11)}^R$ and $A_{N_2(\mathrm{B},v''=0)}^{N_2(\mathrm{C},v'=1)}$ and $\nu_{N_2(C,1)}^R$ are respectively the vibrational transition probabilities and the radiative loss frequencies of the N_2 1+ (11-7) band of the N_2 2+ (1-0) band, k_a and k_c are the rate coefficients of reactions (a) and (c), and $k_{N_2(B,11)}^{Q_M}$ and $k_{N_2(C,1)}^{Q_M}$ are the quenching rate coefficients of the N_2(B,v''=11) and N_2(C,v''=1) levels by M = N_2 or H_2 molecules.

Using the radiative and collisional data of Table 1, the absolute N_2(A) density can be deduced at a given *z* position from eq. 4, using the previously determined *a* value, the absolute N-atom density and the measured $\frac{I_{580nm}^{11-7}}{I_{316nm}^{1-0}}$ band intensity ratio.

Assuming now that, for the same *z* position, a fraction *(1-a)* of the N_2(B,v''=11) level is produced by reaction (b), it comes that :

$$\frac{a}{1-a} = \frac{k_a[N]^2}{k_b[N_2(A)][N_2(X,v'>13)]} \qquad (9)$$

Table 1 – Radiative and collisional rate coefficients used in eqs. (6) and (8).

k_a	$A_{N_2(\mathrm{A},v''=7)}^{N_2(\mathrm{B},v'=11)}$	$\nu_{N_2(B,11)}^R$	$k_{N_2(B,11)}^{Q_{N_2}}$	$k_{N_2(B,11)}^{Q_{H_2}}$
($cm^6\ s^{-1}$)	(s^{-1})	(s^{-1})	($cm^3\ s^{-1}$)	($cm^3\ s^{-1}$)
$1.3\ 10^{-33}$	$7.8\ 10^{4}$	$1.9\ 10^{5}$	$2.8\ 10^{-11}$	$2.8\ 10^{-11}$
[6]	[11]	[11]	[12]	[5]
k_c	$A_{N_2(\mathrm{B},v''=0)}^{N_2(\mathrm{C},v'=1)}$	$\nu_{N_2(C,1)}^R$	$k_{N_2(C,1)}^{Q_{N_2}}$	$k_{N_2(C,1)}^{Q_{H_2}}$
($cm^3\ s^{-1}$)	(s^{-1})	(s^{-1})	($cm^3\ s^{-1}$)	($cm^3\ s^{-1}$)
$4.1\ 10^{-11}$	$1.3\ 10^{7}$	$2.7\ 10^{7}$	$3.3\ 10^{-11}$	$3.2\ 10^{-10}$
[13]	[11]	[11]	[14]	[15]

4 - Results

4.1 – TALIF measurement of N and H atoms absolute densities

Figure 6 compares the absolute N-atom concentrations measured in N_2/(0-5%)H_2 late afterglows at *z* = 50 cm by TALIF and by OES using equation (2).

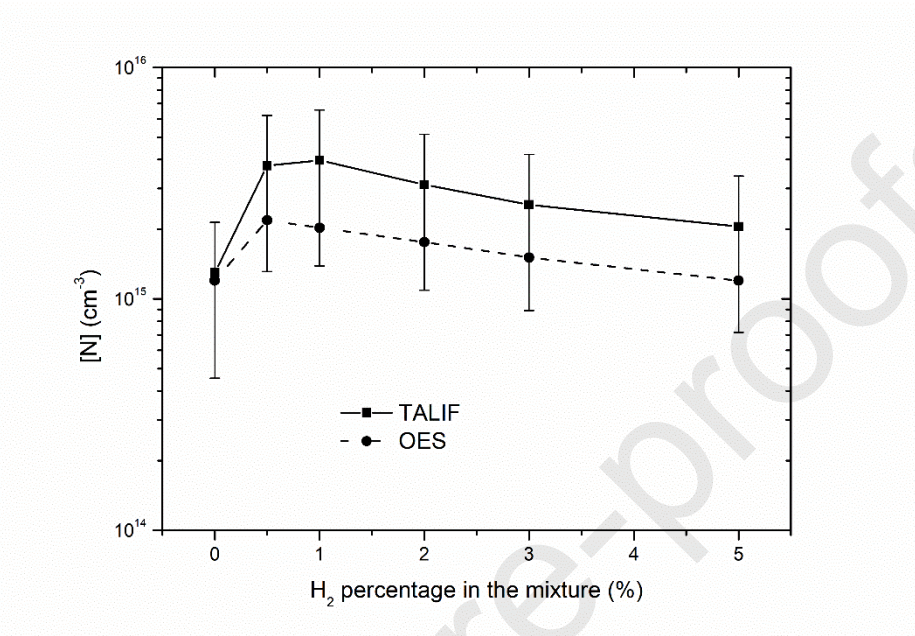

Fig.6. N-atom absolute concentrations obtained by OES and by TALIF in the afterglows of N_2/(0-5%H_2) mixtures. (4 Torr, 0.5 slm, 150 W, z = 50 cm)

Considering the 50% uncertainty in the two-photon excitation cross section ratio ($\frac{\sigma^{(2)}(Kr)}{\sigma^{(2)}(N)}$ = 0.67 ± 0.33, [16]) and the 30% uncertainty generally considered for the OES method [7], a good agreement is found, both methods showing similar relative evolutions and a maximum of the N-atom density in highly diluted mixtures N_2/(0.5-1.0%)H_2, corresponding at least to a doubling of the atomic concentration obtained in pure N_2.

The TALIF method was then applied to the determination of H-atom densities in the N_2/(0-5%)H_2 late afterglows operating in the same conditions (4 Torr, 0.5 slm and 150 W at *z* = 50 cm). The determination of the ground-state atomic hydrogen density was performed using the value of the ratio of two-photon excitation cross sections given by Niemi *et al* [16]: $\frac{\sigma^{(2)}(Kr)}{\sigma^{(2)}(H)}$ = 0.62 ± 0.31.

As shown Figure 7, the H-atom density was found to increase rapidly from 1 10^{14} to 3 10^{14} cm^{-3} when *x* increases from 0.5 to 1%, and reaches a maximum of 4.5 10^{14} cm^{-3} in the N_2/5%H_2 mixture, in correct agreement with the relative variation previously given by Bockel [2]. The corresponding H_2 dissociation rate [H]/2[H_2] shows a pronounced maximum higher than 12% in the N_2/1%H_2 gas mixture, much higher than the N_2 dissociation rate close to 1% obtained in the same conditions.

At *z* = 50 cm, the evolution of the H-atom density with the operating pressure was also measured by TALIF in the N_2/1%H_2 gas mixture. Between 2 and 6 Torr, it was found an almost constant density of 3 10^{14} cm^{-3} (0.5 slm, 150 W).

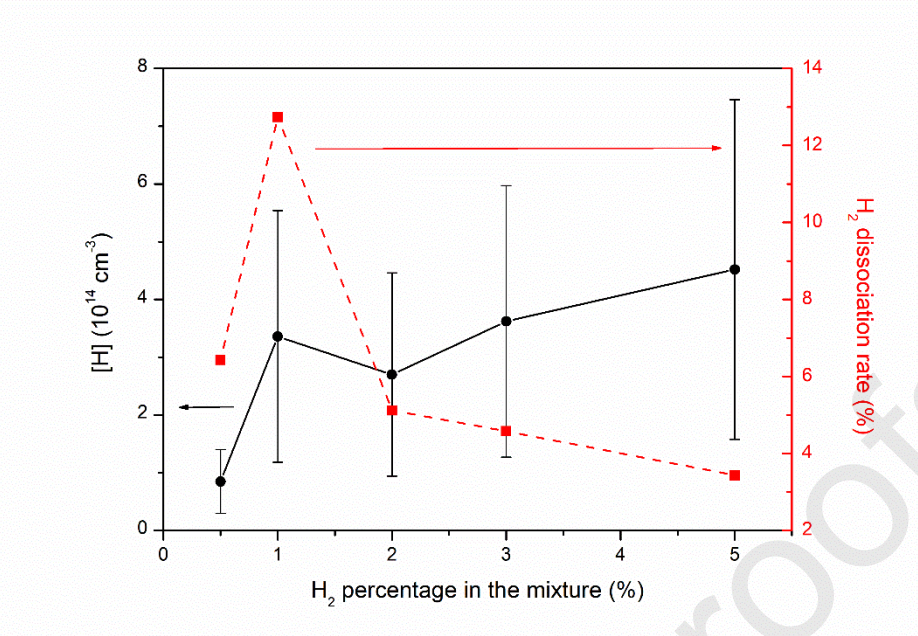

Fig.7. H-atom absolute concentrations obtained by TALIF in the afterglows of N_2/(0.5-5%H_2) mixtures (4 Torr, 0.5 slm, 150 W, z = 50 cm). The corresponding H_2 dissociation rates [H]/2[H_2] are also given.

4.2 – H and NH kinetics in the afterglow region and determination of their absolute densities by OES

NH(X) molecules were already detected by LIF in a DC flowing discharge operating at 2 Torr in a N_2/H_2 mixture [17]. Despite several attempts and a LIF detection threshold as low as 10^9 cm^{-3}, the NH(X) concentration has never been measured in N_2/H_2 afterglows ([2], [17]) while the NH A-X (0-0) band at 336 nm can easily be observed far away from the discharge, as can be seen in the emission spectra reproduced Fig. 5, overlapping with the N_2 2+ (0-0) band emission.

These results suggest that NH can always be created in the ground state NH(X) in the afterglow by the 3-body recombination process:

$$N + H + N_2 \rightarrow NH + N_2 \qquad \text{(d)}$$

with a rate coefficient varying in the literature between the measured value given by Brown (k_d = 5 10^{-32} cm^6 s^{-1}, [18]) and the value k_d =1 10^{-33} cm^6 s^{-1} assumed by Gordiets [19], but is rapidly destroyed by the couple of fast reactions:

$$N + NH \rightarrow H + N_2 \qquad (k_e = 5\ 10^{-11}\ \text{cm}^3\ \text{s}^{-1}, [5]) \qquad \text{(e)}$$

and

$$H + NH \rightarrow N + H_2. \qquad (k_f = 3\ 10^{-11}\ \text{cm}^3\ \text{s}^{-1}, [5]) \qquad \text{(f)}$$

In previous works ([8], [9]), we considered the NH(A) state production in the pink afterglow through the reaction:

$$N_2(X, v > 13) + NH \rightarrow NH(A) + N_2, \qquad \text{(g)}$$

with a rate coefficient k_g = 5 10^{-11} cm^3 s^{-1}, assumed equal to the rate coefficient of the similar $N_2(X,v>13)+N_2(A)$ and $N_2(X,v>13)+N_2^+$ processes [5].

Considering this kinetics and using the pseudo-stationary condition, [H] and [NH] densities are related by:

$$[H] = \frac{k_e[N][NH]}{k_d[N][N_2]+k_f[NH]}. \quad (10)$$

The absolute H atom density can then be derived from the absolute [NH] density obtained through the measured band intensity ratio $I_{580nm}^{11-7}/I_{336nm}^{0-0}$, as:

$$\frac{a\, I_{580nm}^{11-7}}{I_{336nm}^{0-0}} = \frac{K_{580}}{K_{336}} \frac{[N]^2}{[N_2(X,v>13)][NH]}, \quad (11)$$

where I_{336nm}^{0-0} is the measured intensity of the NH A-X (0-0) band (Fig. 5), with:

$$K_{336} = C(336nm) \cdot \frac{hc}{336nm} \cdot A_{NH(X,v''=0)}^{NH(A,v'=0)} \frac{k_g}{\nu_{NH(A,0)}^R + [N_2]k_{NH(A,0)}^{Q_{N_2}} + [H_2]k_{NH(A,0)}^{Q_{H_2}}}. \quad (12)$$

In the above equations, the [N_2(X,v>13)] absolute density is obtained from eq. (9) (using the absolute [N_2(A)] density is deduced from the measured intensity ratio $I_{580nm}^{11-7}/I_{316nm}^{1-0}$) and $C(336nm)$ is the relative spectral calibration factor of the intensity acquisition system at 336 nm. According to Hofzumahaus [20], as the (0-0) band is the main band of the NH A-X system, radiative frequencies $A_{NH(X,v''=0)}^{NH(A,v'=0)}$ and $\nu_{NH(A,0)}^R$ are both equal to 2 10^6 s^{-1}, while the quenching rates of the NH(A,v'=0) level by N_2 and H_2 are respectively equal to 5 10^{-14} cm^3 s^{-1} and 5 10^{-11} cm^3 s^{-1}.

Again, as the NH A-X (0-0) band and the N_2 2+ (0-0) band overlap, half of the minimum intensity between the two peaks is subtracted to the observed NH A-X (0-0) maximum intensity.

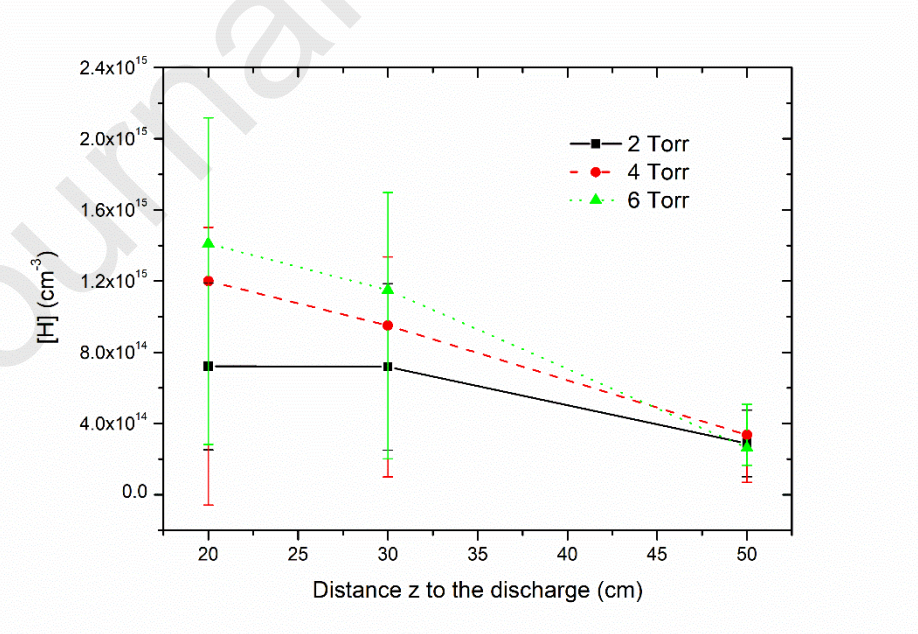

Fig.8. H-atom absolute densities measured by TALIF at different distances z to the discharge in afterglows of a N_2/1%H_2 mixture at pressures of 2, 4 and 6 Torr (0.5 slm, 150 W).

TALIF measurements of the H-atom absolute concentration along the afterglow of a N_2/1%H_2 gas mixture (0.5 slm, 150 W) are shown Figure 8 for pressures of 2, 4 and 6 Torr. It is observed a general decrease of the H-atom density with the distance *z* to the discharge, as N and H atoms are essentially produced in the discharge by direct electron collisions. The H-atom population decrease is more pronounced at 6 Torr, showing the increase of the influence of the three-body reaction (d).

Table 2 gathers band intensity ratios, *a* fraction values, absolute [N_2(X,v>13)] and [N_2(A)] densities obtained from the $I_{580nm}^{11-7}/I_{316nm}^{1-0}$ band intensity ratio and absolute [NH] and [H] densities deduced from eqs. (11) and (10) in the afterglow of a N_2/1%H_2 gas mixture (0.5 slpm, 150 W) at 2 Torr.

Table 2 – Band intensity ratios, a values and absolute species densities obtained in the afterglow of a N_2/1%H_2 mixture operating at 2 Torr (0.5 slm, 150 W). The H-atom density is obtained using eq. (10) with the rates (i) k_d = 5 10^{-32} cm^6 s^{-1} [18] or (ii) k_d = 1 10^{-33} cm^6 s^{-1} [19].

z (cm)	$\frac{I_{580nm}^{11-7}}{I_{316nm}^{1-0}}$	$\frac{I_{580nm}^{11-7}}{I_{336nm}^{0-0}}$	*a*	[N] (10^{14} cm^{-3})	[N_2(X,v>13)] (10^{13} cm^{-3})	[N_2(A)] (10^{10} cm^{-3})	[NH] (10^8 cm^{-3})	[H] (cm^{-3})
20	13	12.6	0.23	6.2	1.6	9.4	61	8.7 10^{13} (i) 8.5 10^{14} (ii)
30	58	110	0.3	6.6	3.0	4.0	3.3	5.1 10^{12} (i) 2.0 10^{14} (ii)
50	490	230	0.6	11	6.0	1.7	1.1	1.7 10^{12} (i) 0.8 10^{14} (ii)

The increase of the *a* fraction with the distance *z* to the discharge shows the increasing weight of reaction (a) in the population of the N_2(B,v'=11) level in the N_2/1%H_2 afterglow. In the intermediary region between the full pink and the full late afterglows (*z* = 20-50 cm), it is observed a decrease of the [N_2(A)] density while the [N_2(X,v>13)] population still increases. It is here shown that this increase conduces to a dissociation enhancement through reaction (h):

$$N_2(X,10 < v' < 26) + N_2(X,10 < v' < 26) \rightarrow N_2(X,v'=0) + N + N \qquad \text{(h)}$$

The NH density rapidly falls down between 20 and 50 cm, to reach concentrations of few 10^8 cm^{-3} lower to the detection threshold of TALIF measurements, which certainly explains why NH cannot be measured by this technique in the afterglow.

By comparing [H] densities given by eq. (10) with the order of magnitude of the TALIF measurements shown Fig. 8, it is deduced that the better agreement is obtained using the rate coefficient k_d = 1 10^{-33} cm^{-3} for reaction (d) [19].

4.3 - Role of N(^{2}D) metastable atoms

It is now considered the role of the N(^{2}D) metastable atoms in the H and NH kinetics.

N(^{2}D) metastable atoms in the afterglow are produced by the following reaction:

$N + N_2(A) \rightarrow N(^2D) + N_2$, (with k_i = 2 10^{-12} cm^3 s^{-1}, [5]) (i)

and destroyed either by quenching:

$N(^2D) + N_2 \rightarrow N(^4S) + N_2$, (with k_j = 2 10^{-14} cm^3 s^{-1}, [19]) (j)

by reactions with H_2 molecules:

$N(^2D) + H_2 \rightarrow NH + H$, (with k_k = 2.3 10^{-12} cm^3 s^{-1}, [5]) (k)

or by collisions with the afterglow tube walls, with a frequency:

$$v^w_{N(2_D)} = \gamma^w_{N(2_D)} < v > /2R \,, \quad (13)$$

where $\gamma^w_{N(2_D)}$ is the N(^{2}D) destruction probability on the quartz tube walls ($\gamma^w_{N(2_D)}$ = 0.1, [21]), $< v >$ is the thermal gas velocity (5 10^4 cm s^{-1} at 300 K) and R is the afterglow tube radius, conducing to $v^w_{N(2_D)}$ = 3 10^3 s^{-1}.

Considering this kinetics, the N(^{2}D) density is given by:

$$\left[N(^2D)\right] = \frac{k_i[N][N_2(A)]}{k_j[N_2]+k_k[H_2]+v^w_{N(2_D)}}. \quad (14)$$

For a 2 Torr pressure, with the N and N_2(A) densities of Table 2, it is found a N(^{2}D) density decreasing from 2.0 10^{10} cm^{-3} for z = 20 cm to 0.6 10^{10} cm^{-3} for z = 50 cm.

Reaction (k) has also to be taken into account as a source term for H-atom production and eq. (10) becomes:

$$[H] = \frac{k_e[N][NH]+k_k\left[N(^2D)\right][H_2]}{k_d[N][N_2]+k_f[NH]}. \quad (15)$$

As $[H_2] = [H_2]_0 - [H]/2$, where $[H_2]_0$ is the initial H_2 density, it is obtained:

$$[H] = \frac{k_e[N][NH]+k_k\left[N(^2D)\right][H_2]_0}{k_d[N][N_2]+k_f[NH]+k_k\frac{[N(^2D)]}{2}}. \quad (16)$$

H-atoms densities calculated with eq. (16) (with k_d = 1 10^{-33} cm^{-3}, [19]) are given Table 3 and compared with TALIF measurements, showing a better agreement than densities obtained with eq. (10) and the strong influence of N(^{2}D) metastable atoms in the H-atom production in N_2/<5%H_2 flowing afterglow through reaction (k).

Table 3 – H-atom densities calculated with eq. (10) and with eq. (16) in a N_2/1%H_2 afterglow in conditions of 2 Torr, 0.5 slm and 150 W, using the rate coefficient k_d = 1 10^{-33} cm^{-3} given in [19] and densities indicated Table 2.

z (cm)	20	30	50
[H] from eq. (10) (in 10^{14} cm^{-3})	8.5	2.0	0.8
[H] from eq. (16) (in 10^{14} cm^{-3})	9.2	4.0	1.9
$[H]_{TALIF}$ (in 10^{14} cm^{-3})	7.2 ± 4.7	7.2 ± 4.7	2.9 ± 1.9

5 - Conclusion

Absolute nitrogen active species densities (N-atom, $N_2(X,v>13)$, $N_2(A)$) have been measured using band intensity ratios in the afterglows of N_2/<5%H_2 discharges and calibration by NO titration. TALIF measurements of the N-atom density were also performed and compared with results derived from OES measurements at different distances from the discharge. A detailed analysis of the NH and H kinetics in the afterglow and the use of the NH A-X (0-0) band emission at 336 nm allowed us obtaining the NH and H absolute densities and to compare this latter with the absolute H-atom concentrations measured by TALIF. A correct agreement is obtained when the rate coefficient of the N + H + N_2 → NH + N_2 3-body recombination is chosen equal to 1 10^{-33} cm^6s^{-1}, as previously estimated by Gordiets [19]. The agreement is further improved when considering the role of N(^{2}D) metastable atoms in H and NH production. In the afterglow, the NH ground state is either rapidly destroyed by reactions with N and H atoms, or excited into the NH(A) state by the reaction $N_2(X,v>13) + NH \rightarrow NH(A) + N_2$, with a rate coefficient equal to 5 10^{-11} cm^3 s^{-1}, explaining why its density, estimated as low as few 10^8 cm^{-3}, cannot be measured by the TALIF technique.

References

[1] H. Malvos, H. Michel, A. Ricard, *J. Phys. D: Appl. Phys.* 27 (1994) 1328.

[2] S. Bockel, J. Amorim, G. Baravian, A. Ricard, P. Stratil, *Plasma Sources Sci. Technol.* 5 (1996) 567.

[3] J. Loureiro, A. Ricard, *J. Phys. D: Appl. Phys.* 26 (1993) 163.

[4] A. Garscadden, R. Nagpal, *Plasma Sources Sci. Technol.* 4 (1995) 268.

[5] E. Tatarova, F.M. Dias, B. Gordiets, C.M. Ferreira, *Plasma Sources Sci. Technol.* 14 (2005) 19.

[6] V. Ferrer, J.P. Gardou, F. Marchal, A. Ricard, J.P. Sarrette*, Eur. Phys. J. D* 76 (2022) 191.

[7] A. Ricard, M. Moisan, S. Moreau, *J. Phys. D: Appl. Phys.* 34 (2001) 1203.

[8] A. Ricard, J. Amorim, M. Abdeladim, J.P. Sarrette, *Plasma Chem. Plasma Proces*s. 40 (2020) 1351.

[9] M. Abdeladim, J.P. Sarrette, J. Amorim, A. Ricard, *Plasma Chem. Plasma Proces*s. 42 (2022) 1201.

[10] S. Bockel, A.M. Diamy, A. Ricard, *Surf. Coat. Technol.* 74-75 (1995) 474

[11] C.O. Laux, C.H. Kruger, *J. Quant. Spectrosc. Radiat. Transfer* 48 (1992) 9

[12] L.G. Piper, *J. Chem. Phys*. 88 (1988) 6911

[13] L.G. Piper, *J. Chem. Phys*. 88 (1988) 231

[14] E. Gat, N. Gherardi, S. Lemoing, F. Massines, A. Ricard, *Chem. Phys. Lett.* 306 (1999) 263

[15] S.V. Pancheshnyi, S.M. Skarikovskaia, A.Y. Starikovskii, *Chem. Phys.* 262 (2000) 349

[16] K. Niemi, V. Schulz-von der Gathen, H.F. Döbele, *J. Phys. D: Appl. Phys.* 34 (2001) 2330

[17] J. Amorim, G. Baravian, A. Ricard, *Plasma Chem. Plasma Proces*s. 15 (1995) 721.

[18] R.L. Brown, *Int. J. Chem. Kinet*. 5 (1973) 663.

[19] B. Gordiets, C.M. Ferreira, M.J. Pinheiro, A. Ricard, *Plasma Sources Sci. Technol.* 7 (1998) 363.

[20] A. Hofzumahaus, F. Stuhl, *J. Chem. Phys.* 82 (1985) 3152

[21] A.V. Volynets, D.V. Lopaev, T.V. Rakhimova, A.A. Chukalovsky, Y.A. Mankelevich, N.A. Popov, A.I. Zotovich, A.T. Rakhimov, *J. Phys. D: Appl. Phys.* 51 (2018) 364002.

In this paper :

- N atoms absolute concentrations were obtained in the afterglows of N_2/(x=0-5%H_2) mixtures using a) optical emission spectroscopy (OES) + NO titration and b) TALIF
- N_2(A) and N_2(X,v>13) metastable densities were also obtained using band intensity ratios
- H atoms absolute concentrations were obtained in the same conditions using TALIF
- For the N_2/1%H_2 mixture, absolute H atoms concentrations were obtained between 2 and 6 Torr at distances to the discharge varying between 20 and 50 cm
- A kinetic scheme relating the H, N, NH and NH(A) species is given, showing that the NH species can be created in the afterglow by the 3-body recombination reaction $N + H + N_2 \rightarrow NH + N_2$ with a rate coefficient of 1.0 10^{-33} cm^6 s^{-1}. This NH species is either rapidly destroyed by reactions with N and H atoms, or excited into the NH(A) state by the reaction $N_2(X,v > 13) + NH \rightarrow NH(A) + N_2$, with a rate coefficient equal to 5 10^{-11} cm^3 s^{-1}.

- The agreement between OES and TALIF measurements is further improved when N(^{2}D) metastable atoms are included in the kinetic scheme.

Author contributions

J.P.S. F.M. and A.R. designed the study and supervised the project. J.P.S. and A.R. developed the theory. V.F., J.P.G., F.M., J.A. and J.P.S. performed the experiments. All the authors discussed the results and contributed to the final manuscript.

Declaration of interests

☒ The authors declare that they have no known competing financial interests or personal relationships that could have appeared to influence the work reported in this paper.

☐ The authors declare the following financial interests/personal relationships which may be considered as potential competing interests: